Journal of Materials, Processes and Environment
May edition. Vol.4. N°1. (2016)
ISSN : 2335-1020

Hydrodynamic and heat transfer performance of shear thinning fluid flow in chaotic geometry under the effect of rheological fluid behavior

T.T. Naas[1], Y. Lasbet[1], A. Benzaoui[2], K. Loubar[3]

[1] Laboratoire de développement en mécanique et Matériaux, Ziane Achour University, Algeria.
[2] Laboratoire Thermodynamique et Systèmes Energétiques (LTSE), Houari Boumedien University, Algeria.
[3] Ecole des Mines de Nantes. Nantes 44307, Cedex 3, France.

ABSTRACT — A numerical analysis of non-Newtonian laminar flow and heat transfer in three-dimensional chaotic geometry has been performed. The steady equations of conservation, mass, Navier-Stokes and energy are solved by using CFD code. The creation entropy in the flow is estimated for a various generalized Reynolds number (Re_g) and for different values of the power law index of the fluid n. The results show that the entropy generation depends to the both heat performances and power law index of the fluid.

Keywords: *C-shaped cannel, Laminar flow, heat transfer, non-Newtonian fluids, entropy generation.*

I.Inroduction

Non-Newtonian fluids flow in complex geometries are widely used in various engineering applications [1]. Experimental and analytical studies have been carried out in such flow systems [2]. Among of the criteria that allow characterizing these systems is the calculation of the entropy created in flow.The entropy is due to both heat transfer and the pressure losses. Mohammad et al [3] investigate the entropy generation in a helically coiled tube in laminar flow with a uniform surface heat flux is imposed. The results showed the effect of different flow conditions such as mass velocity, inlet vapor quality, saturation temperature, and heat flux on contributions of pressure drop and heat transfer in entropy generation. Ko and Ting [4-5] analyzed the entropy production in incompressible laminar shear flows in heated curved rectangular duct. Their results reveal that the addition of rib can effectively reduce the entropy generation from heat transfer irreversibility.
An analytical study of entropy generation for fully developed non-Newtonian flow through microchannels, in which the effects of viscous dissipation on the entropy production were investigated by Hung [6]. Vishal [7] investigated the viscous dissipation effect on entropy generation for non-Newtonian fluids in laminar fluid flow through a microchannelsheated by a uniform surface heat flux. In a recent study of Kefayati [8], heat transfer and entropy generation on laminar natural convection of Non-Newtonian nano-fluids are studied by Finite Difference Lattice Boltzmann Method.

Corresponding author: NAAS Toufik Tayeb, Research field: Mechanecal egineering
Adress. –Djelfa ALGERIA
E-mail: toufiknaas@gmail.com

In the present study, our main aim is to investigate numerically the entropy generations caused by heat transfer and fluid friction as function of the generalized Reynolds and for different values of the power law index ranges from 0.5 to 0.9 in complex geometry with a uniform surface heat flux.

II. Physical model

Figure 1 show the C-Shaped channel geometry, which has been introduced by Liu et al [1] and generated spatially chaotic flows by Beebe [9]. The channel cross-sectionis square (15 cm × 15 cm), the hydraulic diameter D_h is 15 cm andthe unfolded length is equal to 0.135 m.

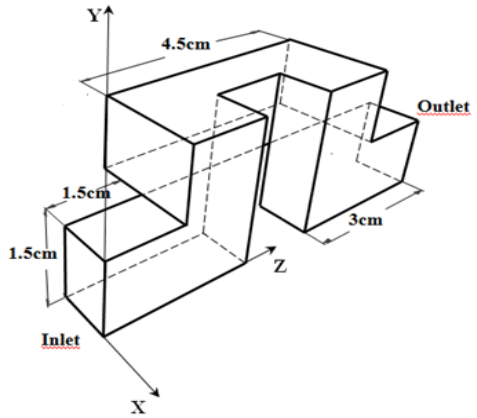

Fig.1 C-shaped channel geometry

III.Analysis

III.1. Non-Newtonian fluid model

In order to model the flow of non-Newtonian fluids,

the purely viscous (i.e., inelastic) non-Newtonian character of the fluid that studied here is represented by Bird et al [10] power-law model for the case of both shear-thinning and Newtonian fluids. The constitutive relation between the shear stress τ (Pa) and the shear rate γ (s−1) can be described by a simple power law expression:

$$\tau = k\gamma^n \qquad (1)$$

Where k (Pa-1) is power-law consistency index and n is the flow behavior index of the fluid.
The nonlinear relationship between the apparent viscosity μ_{app} (N.s .m−2) and the shear rate γ is given by the constitutive equation:

$$\mu_{app} = k\gamma^{n-1} \qquad (2)$$

We will consider five different flow behavior indexes that are associated with shear-thinning ranging from n = 0.5 to 0.9). The consistency index (k) is adapted in each non-Newtonian case in order to give the same generalized Reynolds number asit was considered for the Newtonian flow (Re =$\rho U_i D_h^n/\mu$).This generalized Reynolds number (Reg), can be written for the power-law fluid as [11]:

$$\mathrm{Re_g} = \frac{\rho U_i^{2-n} D_h^n}{\left[8^{n-1}\left(b^* + \frac{a^*}{n}\right)^n k\right]} \qquad (3)$$

Wherea* and b* equal 0.2121and 0.6771 respectively, for square channel, ρdensity of fluid (kg.m−3), and Ui(m/s) is the inlet velocity.

III.2 Entropy generation in laminar flows

The localentropy generation in the laminar flow is given for three dimensional flow as follows [12,14]:

$$S'''_{gen} = \frac{\lambda}{T^2}\left[\left(\frac{\partial T}{\partial x}\right)^2 + \left(\frac{\partial T}{\partial y}\right)^2 + \left(\frac{\partial T}{\partial z}\right)^2\right] + \frac{\mu_{app}}{T}\left[2\left(\left(\frac{\partial u}{\partial x}\right)^2 + \left(\frac{\partial v}{\partial y}\right)^2 + \left(\frac{\partial w}{\partial z}\right)^2\right) + \left(\frac{\partial u}{\partial y} + \frac{\partial v}{\partial x}\right)^2 + \left(\frac{\partial u}{\partial z} + \frac{\partial w}{\partial x}\right)^2 + \left(\frac{\partial v}{\partial z} + \frac{\partial w}{\partial y}\right)^2\right] \qquad (4)$$

The first term on the right-hand side is entropy generation due to heat transfercontribution and the second term is the entropy generation due to pressure losses contribution.So, the total volumetric entropy generation is given by:

$$S'''_{gen} = S'''_{gen,\Delta T} + S'''_{gen,\Delta P} \qquad (5)$$

In orderto characterize the compromise between the entropy generation and the heat transfer, it is worth to follow the non-dimensional entropy generation defined as [12,14]:

$$N_S = \frac{\iiint S'''_g \, dV}{\dot{Q}/T_i} \qquad (8)$$

Better compromise is obtained when NS is lower.
Where V is total volume of the channel,$\dot{Q}$ is the total heat transfer rate and T_i is the inlet temperature.
In addition, in the literature [14], Bejan number is frequently used and it is defined as follows:

$$\mathrm{Be} = \frac{S'''_{gen,\Delta T}}{S'''_{gen,\Delta T} + S'''_{gen,\Delta P}} \qquad (9)$$

The value of Be ranges from 0 to 1. Accordingly, Be=0 and Be=1 are two limiting cases representing the irreversibility is dominated by fluid friction and heat transfer, respectively.

IV. Numerical method and grid independent test

The conservation, Navier-Stokes and energy equations are solved by CFD code to calculate the thermodynamic characteristics of non-Newtonian fluids. The momentum and energy terms are treated with the second order upwind scheme, while the pressure term takes the standard scheme. The gradients on the faces are evaluated with the Node-Based method, i.e., taking the arithmetic average of the nodal values on the face. The double-precision segregated solver is adopted for the computation, and pressure and velocity are coupled with the 'SIMPLE' algorithm. The computations were considered to be converged once all the scaled residuals are less than 10-7 and the global imbalances, representing overall conservation don't exceed 10-5.

To optimise the mesh size, it was necessary to carry out a mesh independence study.This was done by performing a number of simulations with different mesh sizes. The mesh grids are ranging from 30 to 60 nodes in the x, y and z directions for each 0.015 m. The results are presented below for the case of non-Newtonian fluid flow in the C-shaped geometry considering a steady laminar flow, at fixed generalized Reynolds number $\mathrm{Re_g}$= 200 and Power-law index n = 0.5. Figure2 shows the evolutions entropy generation due to heat transfer and entropy generation due to friction factor for various grids. It indicates that the entropy generation is sensitive to the grid mesh except for the mesh densities (50*50*50) and (60*60*60) where no significant difference is seen. As consequence, the (50*50*50) grid is chosen as the optimal grid mesh for the computations.

V. Results and discussions

For understanding the thermodynamic behavior, the evolutions of dimensional entropy generation in the C-shaped channel are presented in figures (3) and (4). Figures (3) and (4) present the evolutions of the entropy generation due to heat transfer and pressure losses respectively with generalized Reynolds number for different value of power law index n ranges from n=0.5 to n=0.9. The entropy generation due to the heat transfer presented in figure (3) decreases with generalized Reynolds number.

We can see that the entropy generation due to the heat transfer depends considerably to the power law index n. At low values of n, the fluid is much viscous and consequently the heat transfer is dominated by the molecular diffusion (conduction mode). For given value of generalized Reynolds number, the $\iiint S'''_{gen,\Delta T} dV$ increases when n decreases. So we can remark that this mode of heat exchange (conduction) enhanced the entropy generation contrary to the convection mode (high value of n).

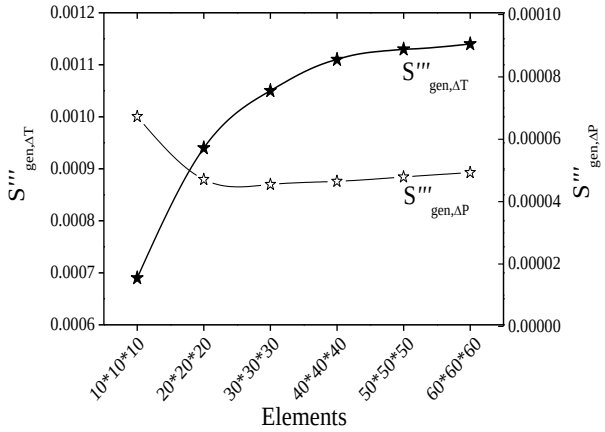

Fig. 2 Entropy generation due to heat transfer and friction factor for different elements in C-shaped channel, for n = 0.5

The entropy generation due to pressure losses presented in figure (4) increases with generalized Reynolds number for all considered values of n. For a considered value of generalized Reynolds number, the entropy generation due to pressure losses increases when n increases contrary to the evolutions of the entropy generation due to the heat transfer. For the same values of the generalized Reynolds number and the power law index n the entropy generation due to pressure losses is smaller compared to the entropy generation created by the heat transfer. Generally, the entropy generation due to the pressure losses is negligible in laminar flow.

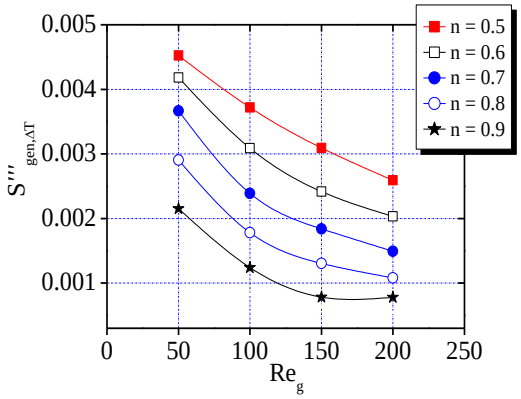

Fig. 3 Evolutions of the entropy generation rate due to heat transfer ($\dot{S}_{gen,\Delta T}$)for different Power-law indexes with various values of Reg.

The evolutions of the global entropy generation $\dot{S}_{gen}$ fordifferent values offlow behavior index n with Re_g have been shown in figures 5.This curve is decreasing with the increasing of both the generalized Reynolds number and power law index n. Because the global entropy generation is proportional to the heat transfer rate, it is interesting to follow the evolution of non-dimensional entropy generation NS defined as the equation 8.

This parameter reflects the better compromise between the entropy creation and the heat transfer rate.For low value of NS the entropy generation is weak compared to the heat transfer rate and the efficient of the geometry is higher.

The evolution of Ns with generalized Reynolds number for various values of the power law index n is presented in figure 6. NS decreases with both generalized Reynolds number and power law index n. This explain that the better compromise (entropy creation-heat transfer) is obtained for low values of n and Reg.In other words, our geometry is more effective when the fluid is Non-Newtonian and the mode of heat transfer is conduction.

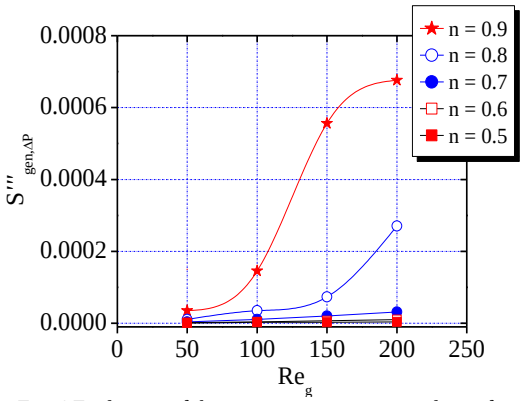

Fig. 4 Evolutions of the entropy generation rate due to friction factor($\dot{S}_{gen,\Delta P}$)for different Power-law indexes with various values of Re_g.

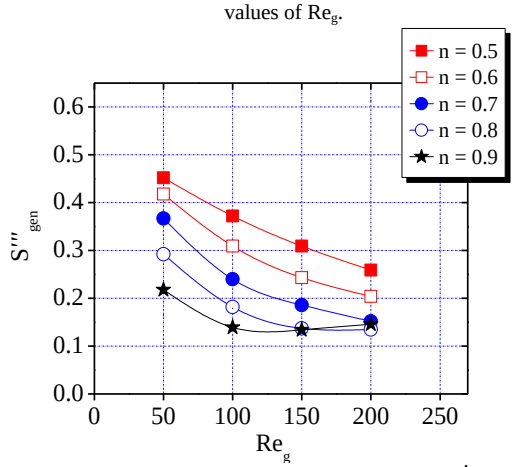

Fig. 5 Evolutions of the global entropy generation rate $\dot{S}_{gen}$ for different Power-law indexes with generalized Reynolds number.

To compare the entropy generation due to the pressure losses with global entropy generation, we present the evolution of Bejan number as function of the generalized Reynolds number for different values of power law index n ranging from 0.5 to 0.9, see figure 7. At low n number and generalized Reynolds number, the entropy generation is due only to the heat transfer. Once the two parameters (n and Reg) increase, the two types of the entropy generation are created concurrently.

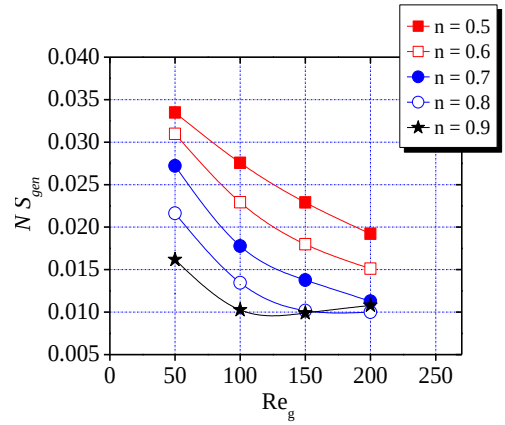

Fig. 6 Evolutions of the global non-dimensional entropy generation rate NS_{gen} for different Power-law indexes.

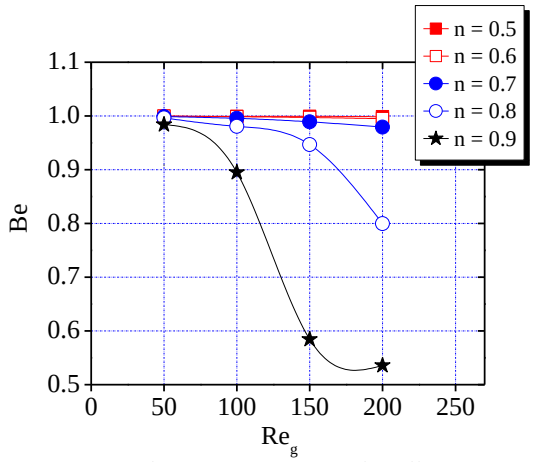

Fig. 7 Evolutions of the Bejan number (Be) for different Power-law indexes with generalized Reynolds number.

VI. Conclusion

This paper deals numerically the creation entropy generation due to the both heat transfer and pressure losses with generalized number and power law index n in complex geometry with imposed surface heat flux density. At low Reg, the entropy generation is dominated by the heat transfer and when the Reg increases the two types of entropy generation are created simultaneous. The efficient of our geometry is higher at both low generalized Reynolds number and power law index n. The optimum case (Reg, n) of our system will be the object in outlook work.

Nomenclature

a*	geometric constant in generalized Reynolds
b*	number, Eq (3)
Be	geometric constant in generalized Reynolds
D_h	number, Eq (3)
K	Bejan number
n	Hydraulic diameter, (m)
Ns	power-law consistency index, (Pa/s)
p	flow behavior index
q"	Non-dimensional entropy generation
Q̇	Pressure, (Pa)
Re	The non-dimensional external heat flux
Re_g	external heat flux, (W/m^2)
$\dot{S}_g'''$	heat transfer rate, (W)
$\dot{S}_{g,\Delta T}'''$	Reynolds number
$\dot{S}_{g,\Delta P}'''$	generalized Reynolds number
T	global entropy generation, (W/ K m^{-3})
T_i	entropy generation due to heat transfer, (W/
u	K^{1}m^3)
U_i	entropy generation due to friction factor, (W/
V	K^{1}m^3)
μ	temperature, (K)
μ_{app}	inlet temperature, (K)
$\dot{\gamma}$	velocity, (m /s)
ρ	inlet velocity, (m /s)
λ	volume, (m^3)
	viscosity, (N s/ m^2)
	apparent viscosity, (Ns/ m^2)
	shear rate, (1/s)
	density, (Kg/m^3)
	thermal conductivity, W/(m K)

References

[1] H. Aref. Stirring by chaotic advection. *J. Fluid Mech, 143-121.1984.*

[2] H. Aref. Order in chaos. *Nature, 401, 756-757.1999.*

[3] Mohammad Ali Abdous, Hamid Saffari, Hasan Barzegar Avval, Mohsen Khoshzat Investigation of entropy generation in a helically coiled tube in flow boiling condition undera constant heat flux, *international journal of refrigeration 60, 2015, 217–233.*

[4] T.H. Ko, Numerical analysis of entropy generation and optimal Reynolds number for developing laminar forced convection in double-sine ducts with various aspect ratios, *International Journal of Mass and Heat Transfer 49 (3-4), 2006, 718–726.*

[5] T.H. Ko, K. Ting, Entropy generation and optimal analysis for laminar forced convection in curved rectangular ducts: a numerical study, *International Journal of Thermal Sciences 45 (2), 2006, 138–150.*

[6] Y.M. Hung Viscous dissipation effect on entropy generation for non-Newtonian fluids in microchannels", International Communications in Heat and Mass Transfer 35, 2008, 1125–1129.

[7] Vishal Anand Slip law effects on heat transfer and entropy generation of pressure driven flow of a power law fluid in a microchannel under uniform heat flux boundary condition, *Energy 76, 2014, 716e732.*

[8] GH.R. Kefayati Simulation of heat transfer and entropy generation of MHD natural convection of non-Newtonian nanofluid in an enclosure, *International Journal of Heat and Mass Transfer 92, 2016, 1066–1089.*

[9] D. Beebe, R. Adrian, M. Olsen, M. Stremler, H. Aref, B. Jo, Passivemixing in micro-channels: fabrication and flow experiments, *MécaniqueInd. 2, 2001, 343–348.*

[10] R.B. Bird. W.E. Stewart. and E.N. Lightfoot.. *Transport Phenomena. Seconded. Wiley, New York 2002.*

[11] A. B. Metzner and J. C. Reed, Flow of Non-Newtonian Fluids -Correlation of the Laminar Transition, and Turbulent-Flow Regions, *1955,AIChE J. 1: 434.*

[12] A. Bejan, Entropy Generation Through Heat and Fluid Flow, *Wiley,New York, 1982.*

[13] P.K. Nag, N. Kumar, Second law optimization of convection heat transfer through a duct with constant heat flux, Int. J. *Energy Res. 13,189, 537–543.*

[14] A. Bejan, Entropy Generation Minimization, *CRC Press, Boca Raton,FL, 199*